CALCULATION OF FAR WINGS OF ALLOWED SPECTRA: THE WATER CONTINUUM

R. H. TIPPING
Department of Physics and Astronomy
University of Alabama
Tuscaloosa, AL 35487

and

Q. MA
Department of Applied Physics
Columbia University and
Institute for Space Studies
Goddard Space Flight Center
New York, NY 10027

ABSTRACT. A far-wing line shape theory based on the binary collision and quasistatic approximations that is applicable for both the low- and high-frequency wings of allowed vibration-rotational lines has been developed. This theory has been applied in order to calculate the frequency and temperature dependence of the continuous absorption coefficient for frequencies up to 10 000 cm^{-1} for pure H_2O and for H_2O-N_2 mixtures. The calculations are made assuming an interaction potential consisting of an isotropic Lennard-Jones part and the leading long-range anisotropic part, and utilizing the measured line strengths and transition frequencies. The results compare well with existing data, both in magnitude and in temperature dependence. This leads us to the conclusion that although dimer and collision-induced absorptions are present, the primary mechanism responsible for the observed water continuum is the far-wing absorption of allowed lines. Recent progress on near-wing corrections to the theory and validations with recent laboratory measurements are discussed briefly.

1. INTRODUCTION

The absorption of radiation by water vapor in the window regions of the Earth's atmosphere is a long-standing problem [1] of great practical as well as theoretical interest [2].

G.C. Tabisz and M.N. Neuman (eds.), Collision- and Interaction-Induced Spectroscopy, 369–381.

In the past few years there have been a number of general review [3-6] concentrating primarily on the experimental characterization of this absorption, which for historical reasons is called the "water continuum", and the interested reader is referred to these reviews for original literature citations. As a result of this extensive work, there is nearly unanimous agreement on the density dependence (quadratic), general agreement on the temperature dependence (strong, negative, at least in the 8-13 μm window for atmospheric temperatures), but considerable disagreement as to the magnitude and physical mechanism responsible for the absorption. Water dimers [7] and polymers [8], collision-induced absorption [9], and the superposition of the far wings of collisionally broadened allowed dipole lines [1] have all been suggested as possible sources of the water continuum. While the first two mechanisms are undoubtedly present and contribute to the absorption in the atmosphere, there is increasing evidence that they are not the primary mechanism.

Within the past decade, substantial progress in calculating the absorption in the far wings of allowed transitions has been made. Starting from the basic formalism of Fano [10] and Davies et al. [11], Rosenkranz [12,13] has developed a quasistatic statistical theory that is applicable in the high-frequency wing of the pure rotational band (the 8-13 μm window). This theory successfully predicted both the magnitude and the strong, negative temperature dependence. A line-by-line generalization of Rosenkranz' theory was proposed by Boulet et al. [14], but because of the extensive computations involved, it has been implemented only for atom-molecule collisions. In a series of recent papers [15-20], Ma and Tipping have eliminated many of the restrictions in the quasistatic theory so that it now constitutes a unified theoretical framework within which one can calculate the magnitude and temperature dependence of the self- and foreign- broadened far-wing absorption.

In the present paper, we briefly review the mathematical formalism and the nature of the approximations made. We then discuss the theoretical line shapes and the resulting absorption coefficient $\alpha(\omega)$ for the case of pure water vapor, and present comparisons with selected experimental data. Finally, we indicate the principal difficulties of the present theory, and discuss possible improvements that are feasible within the current framework.

2. THE GENERAL THEORETICAL FRAMEWORK

For a low-density gas in thermal equilibrium at a

temperature T, binary collisions dominate and one can focus on one absorber molecule and treat the other molecules as a bath. In this case, the absorption coefficient per unit volume $\alpha(\omega)$ at frequency ω is given by the well-known formula

$$\alpha(\omega) = (4\pi^2/3\hbar c)\ n_a\ \omega\ \tanh(\hbar\omega/2kT) \times [F(\omega) + F(-\omega)] \quad , \tag{1}$$

where the spectral density, $F(\omega)$, is given by

$$F(\omega) = \pi^{-1}\ \mathrm{Re}\ \mathrm{Tr} \int_0^\infty e^{i\omega t} \langle \vec{\mu}_a(0) \cdot \vec{\mu}_a(t) \rangle\ dt \ . \tag{2}$$

In this expression, $\vec{\mu}_a(t)$ is the dipole operator of the absorber molecule in the Heisenberg representation and the angular brackets denote the ensemble average over all (one absorber plus all bath molecules) variables. Introducing the total Liouville operator L

$$L = L_0 + L_1 = L^{(a)} + L^{(b)} + L_1 \ , \tag{3}$$

where L_0 is the unperturbed part describing the absorber a and bath molecules b, and L_1 corresponds to the interaction between them, the spectral density can be written in the form

$$F(\omega) = \frac{1}{\pi}\ \mathrm{Re}\ \mathrm{Tr} \int_0^\infty e^{i\omega t}\ \{\vec{\mu}_a(0) \cdot e^{-iLt}\ \rho\ \vec{\mu}_a(0)\} dt \ , \tag{4}$$

where ρ is the density operator. As shown in [18], e^{-iLt} can be approximated by

$$e^{-iLt} = e^{-iL_0 t}\ e^{-iL_1 t} \times \{1 - i \int_0^t dt_1\ L'_1(t_1) + \cdots\} \quad , \tag{5}$$

where

$$L'(t) = e^{iL_1 t}\ e^{iL_0 t}\ L_1\ e^{-iL_0 t}\ e^{-iL_1 t} - L_1 \ . \tag{6}$$

Substituting Eq. (5) in Eq. (4), the spectral density can be represented by the expansion

$$F(\omega) = F_0(\omega) + F_1(\omega) + \ldots \tag{7}$$

where $F_1(\omega)$ is the first-order correction term resulting

from the non-commutation of L_0 and L_1. Within the quasistatic framework, $F_0(\omega)$ and $F_1(\omega)$ can be expressed in terms of symmetrized line-shape functions [15-20] $\hat{\chi}_{ij}^{(0)}(\omega)$ and $\hat{\chi}_{ij}^{(1)}(\omega)$, respectively, where the transitions are labeled by subscripts i and j; in principle, these can be calculated from the interaction potential $V(\vec{r})$ if we assume it to be of the form

$$V(\vec{r}) = V_{iso}(r) + V_{aniso}(\vec{r}) \quad , \tag{8}$$

and only consider the leading long-range part of the anisotropic potential (dipole-dipole for H_2O-H_2O or dipole-quadrupole for H_2O-N_2). This approximation simplifies the theoretical expressions for the line shape functions but limits the accuracy of the results. Recently, we have generalized the theory to incorporate multi-component potentials, but have not yet carried out calculations for H_2O [20]. To reduce the computation time required, one usually introduces band-average line shape functions $\hat{\chi}^{(0)}(\omega)$ and $\hat{\chi}^{(1)}(\omega)$; that is, the same line shape is assumed for every line in a given vibrational band. Because the derivations as well as the theoretical expressions for the individual and band-averaged symmetrized line shape functions are rather complicated, they are not given here but can be found in [15-20].

Using the results for the spectral densities expressed in terms of the symmetrized line shape functions, one can write the absorption coefficient $\alpha(\omega)$ in the form

$$\alpha(\omega) = n_a \sum_{\omega_{ij}>0} S_{ij} \frac{\omega \sinh(\hbar\omega/2kT)}{\omega_{ij} \sinh(\hbar\omega_{ij}/2kT)}$$

$$\times \pi^{-1} \left(\frac{1}{(\omega - \omega_{ij})^2} \hat{\chi}_+(\omega - \omega_{ij}) \right.$$

$$\left. + \frac{1}{(\omega + \omega_{ij})^2} \hat{\chi}_-(\omega + \omega_{ij}) \right) \quad , \tag{9}$$

where

$$\hat{\chi}_\pm(\omega) = \hat{\chi}_\pm^{(0)}(\omega) + \hat{\chi}_\pm^{(1)}(\omega) \tag{10}$$

and S_{ij} are the usual line strengths. The subscripts $\pm$ indicate the positive- or negative-resonance line shape functions [15-17]; these have a different functional dependence on the frequency and reflect the fact that neither the individual nor the band average line shape functions are symmetric functions. If the differences

between the positive- and negative-resonance line shape functions are neglected, one gets the band average line shape function introduced by Rosenkranz [12,13], which is written without a subscript.

The results for $\hat{\chi}^{(0)}(\omega)$, $\hat{\chi}^{(1)}(\omega)$, and $\hat{\chi}(\omega)$ are shown in Fig. 1 for pure water calculated at T = 296 K. If the lines were Lorentzian, these curves would be horizontal lines whose intercepts would be the corresponding half-widths. However, as can be seen from the figure, the shapes are super-Lorentzian out to approximately 200 cm^{-1} from the line center, after which they fall off very rapidly with frequency.

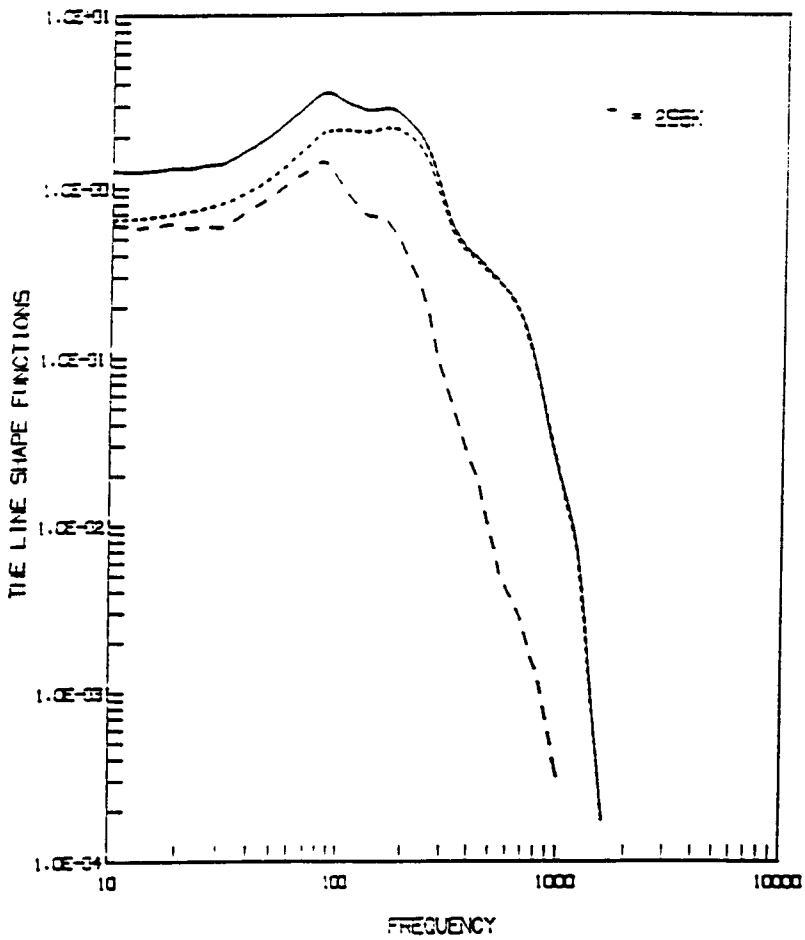

Figure 1. The line shape functions (in units of cm^{-1} atm^{-1}) as a function of frequency ω (in units of cm^{-1}) calculated at T = 296 K. The dotted curve is the band-average line shape function without the near-wing correction, the dashed curve is the near-wing correction, and the solid curve is the total.

Furthermore, the correction term is significant between 10 and 80 cm^{-1}, after which it is negligible. For displacements less than 10 cm^{-1} it is comparable to or even greater than the leading term, but in this region the quasistatic approximation used to calculate the line shape functions is not valid [19].

By excluding any contribution from frequency displacements less than 25 cm^{-1}, one can calculate the absorption coefficient using Eq. (9); the results are shown in Fig. 2 for T = 296 K. One can clearly see that the magnitude of the far-wing contribution to the absorption varies over 6 decades in the frequency region 0-10 000 cm^{-1}.

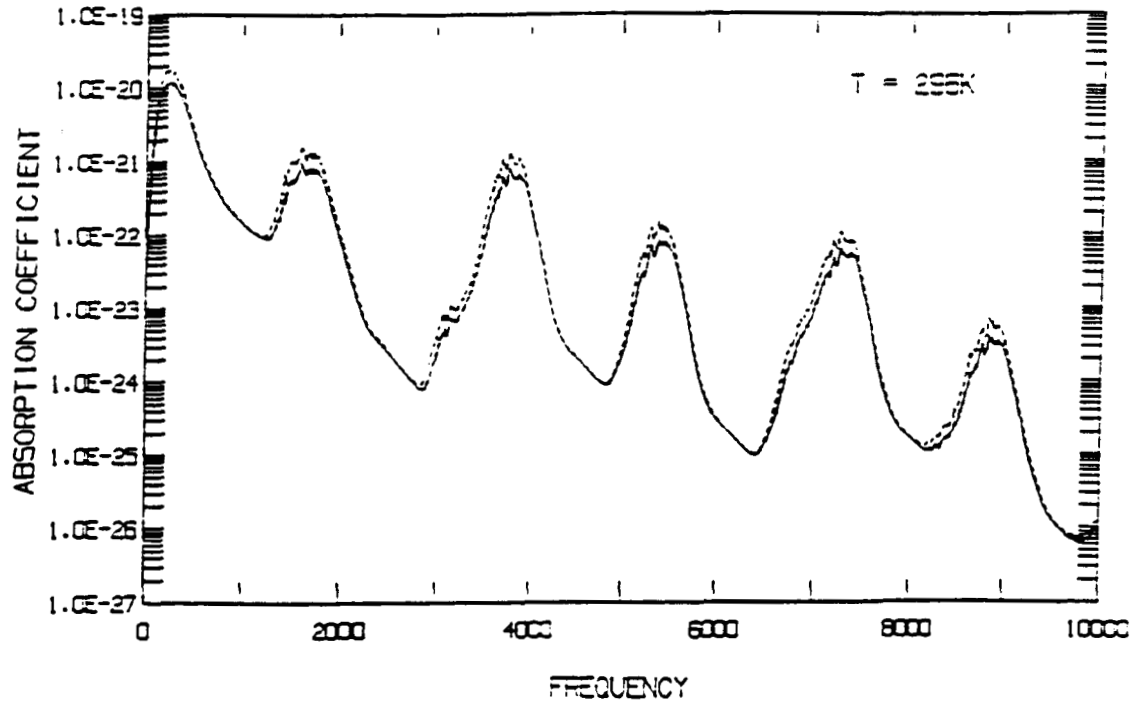

Figure 2. The absorption coefficient $\alpha(\omega)$ (in units of cm^2 $molecule^{-1}$ atm^{-1}) as a function of frequency ω (in units of cm^{-1}) calculated at T = 296 K; the solid line is the result using two symmeterized line shape functions, while the dotted line is the result using the average line shape function.

3. COMPARISONS BETWEEN THEORY AND EXPERIMENT

In order to illustrate the accuracy of the calculations, we present some comparisons between theory and experiment; more comparisons are given in [15-19]. In Fig. 3 we show results for the 300 $cm^{-1} < \omega < 1100$ cm^{-1} region at T = 296 K. Similar results obtain for other temperatures in this region and for other spectral regions, although the agreement is not as good as that shown. However, in these other spectral regions, the continuum contribution is much weaker and the corresponding experimental uncertainties are accordingly larger.

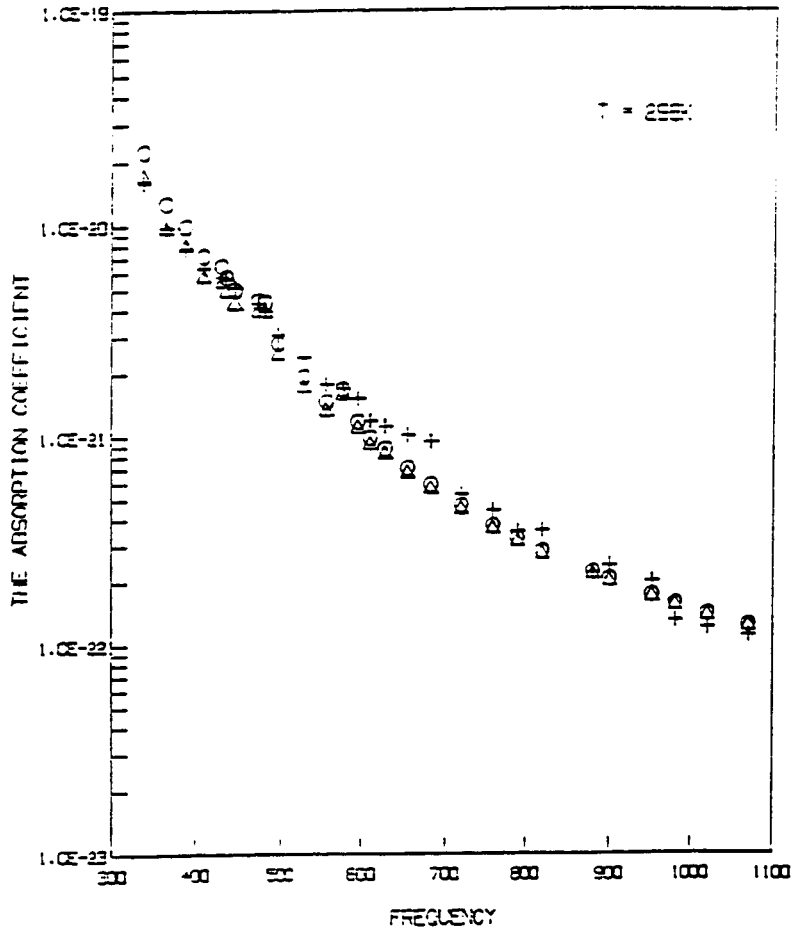

Figure 3. The absorption coefficient $\alpha(\omega)$ (in units of cm^2 $molecule^{-1}$ atm^{-1}) as a function of frequency for 300 $cm^{-1} < \omega < 1100$ cm^{-1} at T = 296 K. The experimental values of Burch et al. [21] are denoted by +, while o and ▲ correspond to the theoretical results obtained without and with the near-wing corrections, respectively.

Furthermore, to obtain the experimental continuum, one has to subtract out the contributions from nearby lines, and different authors use different methods (i.e., different cutoff displacement and/or different line shape functions to represent the central parts of the lines). Nevertheless, as can be inferred from these comparisons, there is generally good agreement in the magnitude of the absorption.

In Fig. 4 we compare the measured and observed temperature dependence. Although the magnitude of the theoretical continuum is less than that observed, the shape is in good agreement.

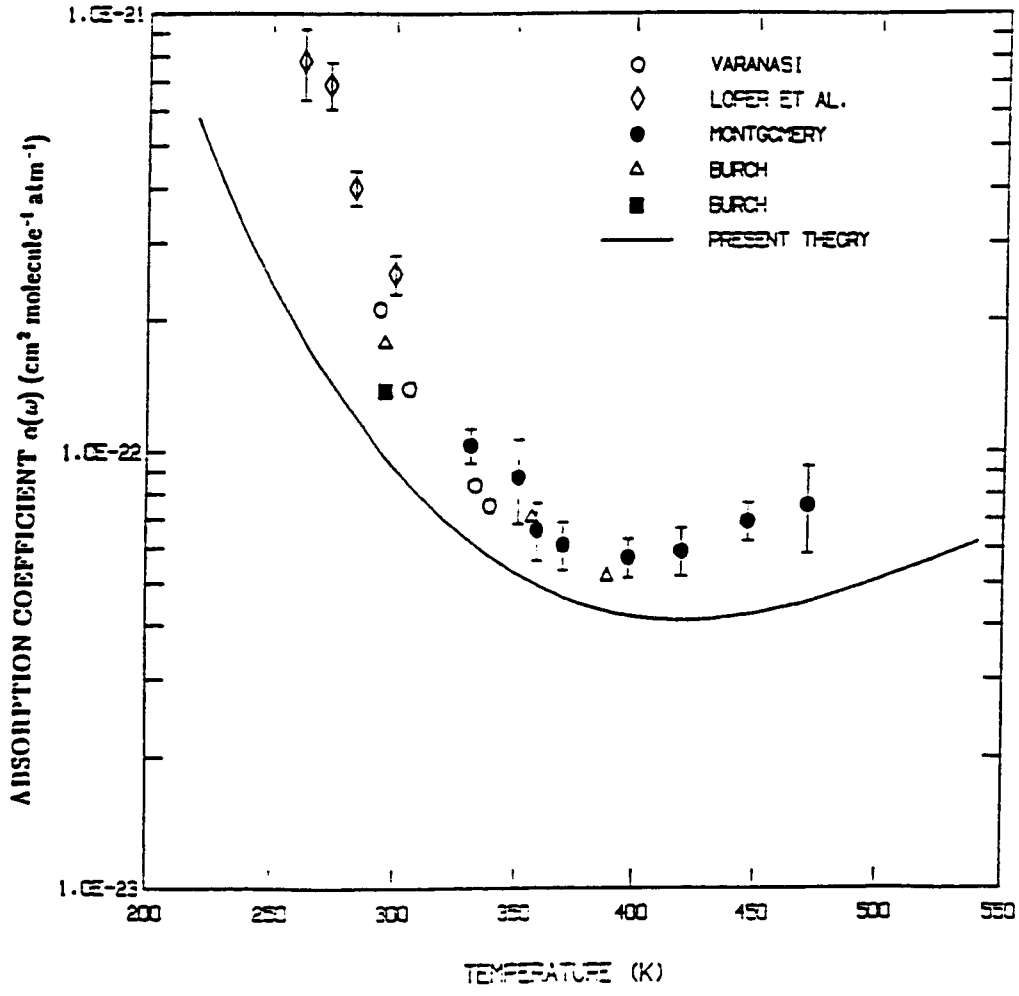

Figure 4. Comparison between the theoretical temperature dependence and various laboratory data: ◇ Loper et al. [22]; • Montgomery [23]; Δ Burch et al. [21]; ■ Burch data, cited by Roberts et al. [24], all for $\omega \cong 1203\ cm^{-1}$; o Varanasi [4] for $\omega \cong 1000\ cm^{-1}$.

We note that for atmospheric temperatures, there is a strong, negative temperature dependence, but this dependence weakens as T increases so that for T > 400 K, the dependence becomes weakly positive. This latter behavior is in sharp disagreement with the exponential decrease one would expect from dimer absorption.

In the comparisons shown above and those not shown but published previously in [15-19], there are no adjustable parameters except the Lennard-Jones parameters describing the isotropic part of the interaction potential. These can, in principle, be determined from other types of measurements, but in our previous calculations, we have adopted the same potential as reported by Rosenkranz [12,13]

$$V_{iso}(r) = C\ \sigma^{-6}\ [(\sigma/r)^{48} - (\sigma/r)^{6}] \qquad (11)$$

where $C/k = 8 \times 10^5$ Å^6 K, and $\sigma = 3.13$ Å. Recently we have carried out calculations in the 700 cm^{-1} to 1300 cm^{-1} frequency region for comparison with accurate experimental data of Kulp [25]. In Fig. 5 we plot the experimental transmission spectrum along with a line-by-line synthesis including the theoretical continuum absorption that is shown separately as well. This was calculated using a 6-12 Lennard-Jones isotropic potential

$$V_{iso}(r) = 4\epsilon\ [(\sigma/r)^{12} - (\sigma/r)^{6}] \qquad (12)$$

with $\epsilon/k = 600$ K and $\sigma = 3.12$ Å; this potential is about 8 % deeper than that in Eq. (11) and significantly wider. From the difference between the experimental data and the model plotted in the lower part of the figure, one can see that there is no systematic difference and the overall agreement is very good.

4. DISCUSSION AND CONCLUSIONS

The results discussed in the previous section for the line shape functions and continuum absorption coefficient (together with more extensive results given in [15-19]) clearly show that the far-wing absorption resulting from an interacting pair of water molecules can account for both the magnitude and the temperature dependence of the observed continuum. This absorption has been calculated by making the following approximations. 1) Only binary collision are considered; for low density gases, this approximation is certainly valid in the wings of the lines. 2) The quasistatic approximation is used; by introducing the

Liouville formalism, the Fourier transform in the spectral density is carried out formally and time does not appear explicitly. The trace over the translational degrees of freedom is replaced by an integration over the separation r between the centers of mass of the colliding pair using the pair potential as a weighting function; the integrand is the matrix elements of the resolvent operator pertaining to the anisotropic interaction which must be diagonalized. Because of this, only one term with a specific spherical symmetry was treated; if more than one term is important, other nonessential approximations can be introduced in order to make the problem tractable [20].

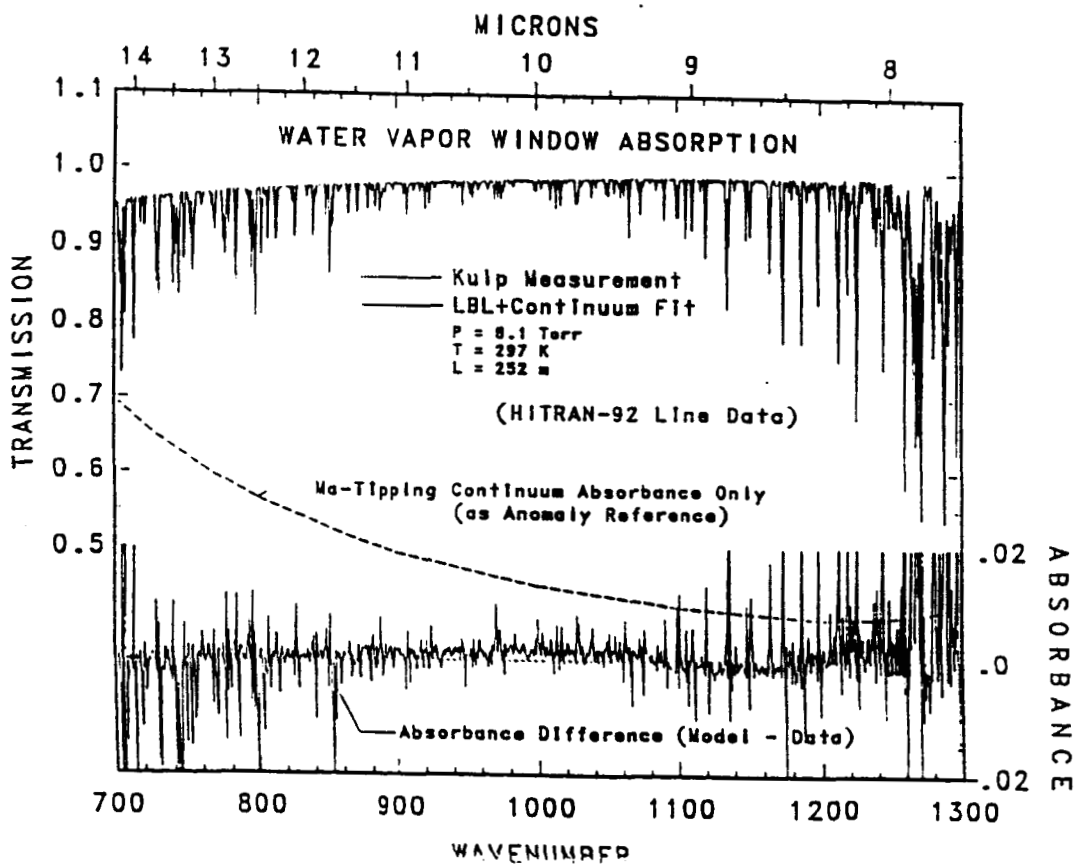

Figure 5. The water vapor transmission spectrum in the 700 cm^{-1} - 1300 cm^{-1} spectral region measured at a pressure of 8.1 torr at T = 297 K using a path length of 252 m [25]. The dotted curve represents the measurements while the solid curve is a synthetic spectrum calculated by a line-by-line method using 92 HITRAN molecular data [26] and the theoretically calculated continuum which is shown separately. The difference in absorbance between the model and the data is plotted in the lower part of the figure.

3) Other approximations such as the band average approximation have been introduced for computational simplicity; these could be avoided if need be, but in light of the other approximations and the extra computation time required, this is not warranted at present. 4) As indicated above, we have only considered simple Lennard-Jones models for the isotropic potential. Other more accurate models or even numerical potentials could be easily incorporated within the present framework. 5) When comparing calculated spectra with experiment (cf. Fig. 5) the effects of the local lines must of course be included. To do this, one has to assume some profile for the absorption near the line center and extrapolate to the near wings (say to 10 or even 25 cm^{-1}). In this intermediate region, neither the impact nor the quasistatic theory is applicable and the true line shape is not known. By including the near-wing effects represented by the spectral density term $F_1(\omega)$, this extrapolation is reduced although the basic problem remains. For the window region around 1000 cm^{-1} this problem is not crucial, but closer to a band center, it can be important [19].

In conclusion, we note that much progress on the theoretical calculation of the far wings of allowed lines has been made. The far-wing absorption is the primary mechanism responsible for the water continuum and this is described reasonably well within the framework of the present theory. However, improvements to the theory in order to calculate the absorption due to the near wings of spectral lines, the use of multi-component anisotropic potentials [20] and more accurate isotropic potential models, and the possible inclusion of other mechanisms (for instance, interferences effects between allowed and induced dipole moments) are needed. Finally, we would like to stress the need for more accurate experimental data (laboratory and atmospheric) that can be used to assess the accuracy of the theoretical results.

ACKNOWLEDGMENTS

The authors would like to thank Dr. T. J. Kulp for providing his water spectral data prior to publication, and Drs. A. Lacis and B. Carlson for their assistance in calculation the line-by-line synthetic spectrum. This work was supported in part by the Department of Energy Interagaency Agreement under the Atmospheric Radiation Measurement Program, and in part by NASA VDAP Grant number NAGW-3875.

REFERENCES

1. Elsasser, W. M. (1938) Ap. J. 87, 497-507 (1938).

2. Deepak, A, Wilkerson, T. D., and Runke, L. H., editors (1980) Atmospheric Water Vapor, Academic Press, New York.

3. Hinderling, J., Sigrist, M. W., and Kneubuhl, F. K. (1987) Infrared Phys. 27, 63-120.

4. Varanasi, P. (1988) J. Quant. Spectrosc. Rad. Transfer 40, 169-175.

5. Grant, W. B. (1990) Appl. Opt., 29, 451-462.

6. Thomas, M. E. (1990) Infrared Phys., 30, 161-174.

7. Penner, S. S., and Varanasi, P. (1967) J. Quant. Spectrosc. Radiat. Transfer, 7, 687-690 ; Suck, S. H., Wetmore, A. E., Chen, T. S. and Kassner, J. L. (1982) App. Opt, 21, 1610-1614.

8. Carlon, H. R. (1982) Infrared Phys. 22, 43-49.

9. Rich, N. H., and McKellar, A. R. W. (1976) Can. J. Phys. 54, 486; Hunt, J. L., and Poll, J. D. (1986) Mol. Phys. 59, 163.

10. Fano, U. (1953) Phys. Rev. 131, 259-268.

11. Davies, R. W., Tipping, R. H., and Clough, S. A. (1982) Phys. Rev. A26, 3378-3394.

12. Rosenkranz, P. W. (1985) J. Chem. Phys. 83, 6139-6144.

13. Rosenkranz, P. W. (1987) J. Chem. Phys. 87, 163-170.

14. Boulet, C., Boissoles, J., and Robert, D. (1988) J. Chem. Phys. 89, 625-634.

15. Ma, Q., and Tipping, R. H. (1991) J. Chem. Phys. 95, 6290-6301.

16. Ma, Q., and Tipping, R. H. (1992) J. Chem. Phys. 96, 8655-8663.

17. Ma, Q., and Tipping, R. H. (1992) J. Chem. Phys. 97, 818-828.

18. Ma, Q., and Tipping, R. H. (1994) J. Chem. Phys. 100, 2537-2546.

19. Ma, Q., and Tipping, R. H. (1994) J. Chem. Phys. 100, 5567-5579.

20. Ma, Q., and Tipping, R. H. (1994) J. Chem. Phys., to be published.

21. Burch, D. E., Gryvnak, D. A., and Pembrook, J. D. (1971) AFCRL-TR-71-0124; Burch, D. E., Gryvnak, D. A., and Gates, F. J. (1974) AFCRL-TR-74-0337; Burch, D. E., Gryvnak, D. A., and Pembrook, J., D. (1975) AFCRL-TR-75-0420; Burch, D. E. (1982) AFGL-TR-81-0300; Burch D. E., and Alt, R. L. (1984) AFGL-TR-84-0128; Burch, D. E. (1985) AFGL-TR-85-0036.

22. Loper, G. L., O'Neill, M. A., and Gelbawachs, J. A. (1983) Appl. Opt. 23, 3701-3710.

23. Montgomery, G. P. (1978) Appl. Opt. 17, 2299-2303.

24. Roberts, R. E., Selby, J. E. A., and Biberman, L. M. (1976) Appl. Opt. 15, 2085-2090.

25. Kulp, T. J., private communication.

26. Rothman, L. S., Gamache, R. R, Tipping, R. H., Rinsland, C. P., Smith, M. A. H, Benner, D. C., Devi, V. M., Flaud, J.-M., Camy-Peyret, C., Perrin, A., Goldman, A., Massie, S. T., Brown, L. R., and Toth, R. A. (1992) J. Quant. Spectrosc. Rad. Transfer 48, 469-507.